Eur. Phys. J. D **43**, 233–236 (2007)
DOI: 10.1140/epjd/e2007-00106-9

THE EUROPEAN PHYSICAL JOURNAL D

Electronic structure of dendrimer-encapsulated Au nanocluster

M. Imamura[1,a], T. Miyashita[2], A. Tanaka[1,2], H. Yasuda[1,2], Y. Negishi[3], and T. Tsukuda[3]

[1] Department of Mechanical and Systems Engineering, Kobe University, Nada-ku, Kobe 657-8501, Japan
[2] Department of Mechanical Engineering, Kobe University, Nada-ku, Kobe 657-8501, Japan
[3] Research Center for Molecular-Scale Nanoscience, Institute for Molecular Science, Okazaki, Aichi 444-0867, Japan

Received 26 July 2006 / Received in final form 1st November 2006
Published online 24 May 2007 – © EDP Sciences, Società Italiana di Fisica, Springer-Verlag 2007

Abstract. We have carried out optical and X-ray photoemission studies of the dendrimer-encapsulated Au nanoclusters. The dendrimer-encapsulated Au nanoclusters are prepared by the chemical reduction of Au ions loaded within the dendrimer templates. Photoluminescence spectrum of the dendrimer-encapsulated Au nanoclusters with diameter of about 1.0 nm shows the visible luminescence centered at about 2.8 eV. In addition, we have measured the nanocluster-size dependent photoemission spectra in the valence-band region. From line shape analysis of Au $4f$ X-ray photoemission spectra, Au $4f$ core-level spectra of the dendrimer-encapsulated Au nanoclusters reflect the size dependent chemical-states. From these results, we discuss electronic structures and chemical states of the dendrimer-encapsulated Au nanoclusters.

PACS. 73.22.-f Electronic structure of nanoscale materials: clusters, nanoparticles, nanotubes, and nanocrystals – 81.07.Pr Organic-inorganic hybrid nanostructures

1 Introduction

Metal-organic hybrid nanoclusters are attracted much attention, since they exhibit distinct optical and electronic properties found in neither bulk nor molecule/atom [1,2]. Recently, the synthesis of the highly monodispersed metallic nanoclusters encapsulated within the dendrimer has been reported by several groups [3–5]. The diameters of these dendrimer-encapsulated metallic nanoclusters are uniform and very small, since the diameters of the dendrimer-encapsulated Au nanoclusters are defined by a size of the internal space of the dendrimer template. Furthermore, these nanoclusters can be easily controlled their solubility, reactivity, and nanocluster-substrate interaction through exchanging the molecule structure and terminal groups on the dendrimer periphery. Therefore, these properties are expected to be suitable for the future applications such as drug delivery, biosensing, and catalysis. In order to elucidate their intriguing properties and to develop the future applications, it is necessary to characterize their detailed electronic structures. In this article, we synthesized the Au nanoclusters encapsulated within 1.5th generation sodium calboxylate-(G1.5-COONa-) terminated polyamidamine (PAMAM) dendrimers, and have performed the optical and photoemission spectroscopic studies of dendrimer-encapsulated Au nanoclusters. From these results, we discuss the electronic structures and chemical states of the dendrimer-encapsulated Au nanoclusters.

2 Experiment

Dendrimer-encapsulated Au nanoclusters were prepared by loading Au ions into dendrimers and subsequent chemical reduction.Gold chloride was mixed with methanol solution of G1.5-COONa-PAMAM dendrimer with vigorously stirring for 1 hour in order to sequester the Au ion into dendrimers. Equivalent sodium borohydride was added into the reaction vial as a reduction agent with another 1 hour stirring. The obtained nanocluster solution was dried, and dissolved into an aqueous solution. The nanocluster solution was ultrafilterated with a centrifugation for several times in order to remove the base and to improve the size distribution. Finally, we obtained two kinds of Au nanocluster samples with different size distributions.

We performed the optical spectroscopic measurements and the X-ray photoemission (XPS) measurements. For the XPS measurements, the synthesized dendrimer-encapsulated Au nanoclusters aqueous solution were dried, and dissolved into the methanol solvent. After that, these obtained nanoclusters were supported on the HOPG substrates by evaporating the solvent (methanol) from the solution of the dendrimer-encapsulated Au nanoclusters on the single-crystalline highly oriented pyrolytic graphite

[a] e-mail: 032d811n@stu.kobe-u.ac.jp

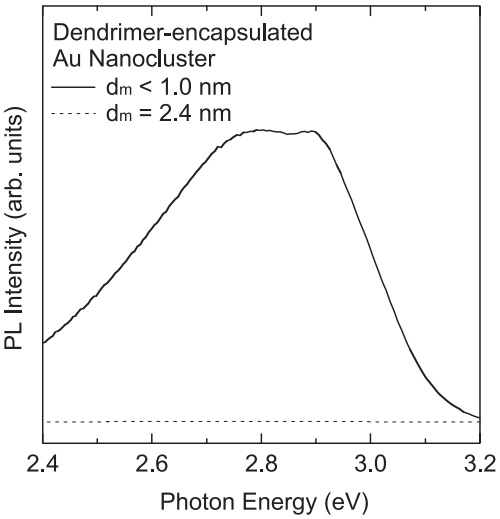

Fig. 1. Photoluminescence spectra of the dendrimer-encapsulated Au nanoclusters in aqueous solution, measured with excitation energy of 3.2 eV.

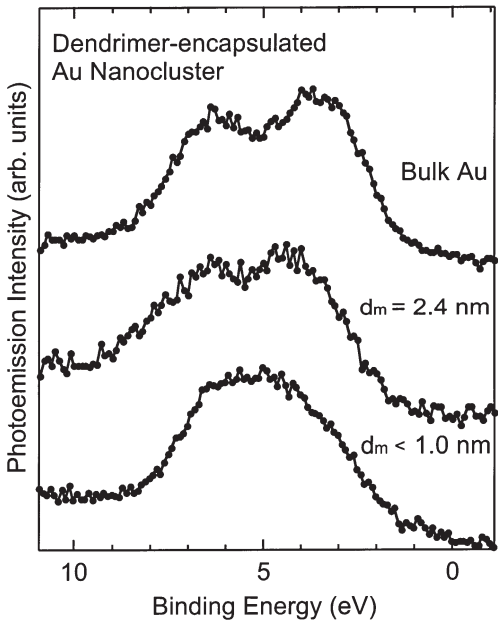

Fig. 2. Valence-band X-ray photoemission spectra of dendrimer-encapsulated Au nanoculusters supported on the HOPG substrates measured with the Mg$K\alpha$ line ($h\nu$ = 1253.6 eV) at room temperature. The top spectrum shows the valence-band photoemission spectrum observed for bulk Au polycrystallite.

cleaved surface in a nitrogen-filled glove bag directly connected to the ultrahigh-vacuum photoelectron spectrometer. Then the Au nanocluster samples were transferred into the photoemission analysis chamber without exposure to air. The XPS measurements were performed using the angle-integrated photoelectron spectrometer with Mg$K\alpha$ line ($h\nu$ = 1253.6 eV) as the excitation source at room temperature.

3 Results and discussion

The size distributions and shapes of the synthesized dendrimer-encapsulated Au nanoclusters were observed by the transmission electron microscopy (TEM). The mean diameter and standard deviation of larger nanocluster sample are 2.4 nm. From TEM micrograh dendrimer-encapsulated Au nanoclusters show the spherical shape, and each nanoclusters are separates from neighboring nanoclusters, indicating that the synthesized nanoclusters are well stabilized by the dendrimer templates. On the other hand, we could not observed the another nanocluster sample due to its cluster size smaller than the spatial resolution of TEM we used. Thus, the nanocluster size of the Au nanocluster is considered to be less than 1.0 nm.

Figure 1 shows the photoluminescence spectra of the dendrimer-encapsulated Au nanoclusters in aqueous solution, measured at room temperature. Both photoluminescence spectra were measured with excitation photon energy of 3.2 eV. As shown in Figure 1, it is found that the dendrimer-encapsulated Au nanoclusters with the diameter of 2.4 nm shows no photoluminescence, however, the dendrimer-encapsulated Au nanoclusters with mean diameter of about 1.0 nm show the strong visible photoluminescence centered at approximately 2.8 eV photon energy. Since the dendrimer-encapsulated Au nanoclusters shows with the diameter of 2.4 nm that involves the dendrimer shows no distinct photoluminescence, the contribution from the dendrimer molecules to the photoluminescence spectrum is considered to be negligible. Therefore, the photoluminescence from the dendrimer-encapsulated Au nanoclusters with diameter of about 1.0 nm is attributed to that from the Au nanocluster itself. Their photoluminescence of the dendrimer-encapsulated Au nanocluster with diameter of about 1.0 nm might be new visible optical transition that results from the modified electronic-structure due to quantum confinement effect.

Figure 2 shows the XPS spectra in the valence-band region of present dendrimer-encapsulated Au nanoclusters. The photoemission spectrum observed for bulk Au polycrystalline is also shown for a comparison in Figure 2. The broad features around 3−8 eV binding energy are assigned to Au 5*d*-derived states. These Au 5*d*-features dominate the valence-band spectra, since their cross sections are higher than the *sp* electronic states of Au. As shown in Figure 2, Au 5*d*-derived features of the bulk Au crystalline and Au nanocluster with mean diameter of 2.4 nm display the well-defined *d*-band doublets. However, the apparent spin-orbit splitting of Au nanocluster with the mean diameter of 2.4 nm is narrower than that of bulk crystallite. On the other hand, the *d*-band doublet in the XPS spectrum of Au nanocluster with the diameter less than 1.0 nm is not clearly observed. It has been well established that the noble-metal *d*-*d* interaction in bulk crystallite is very strong and Au 5*d* bandwidth and the associated apparent spin-orbit splitting decreases with decreasing of the coordination number of the nearest atom [6]. The apparent spin-orbit splitting is described

as $\Delta_{5d} = (\Delta^2_{band} + \Delta^2_{s.o.})^{1/2}$, where Δ_{band} is the band broadening contribution and $\Delta_{s.o.}$ is the true atomic spin-orbit splitting. The band-broadening contribution Δ_{band} decreases with the number of nearest neighbors. Since the surface atoms have the smaller number of the nearest neighbor than inner atom in bulk crystallite, and therefore, the surface d-derived band and the associated apparent spin-orbit splitting are narrowed compared with that of bulk crystallite. Since the relative number of surface to inner atoms in nanocluster increases with decreasing the nanocluster size, the apparent spin-orbit splitting of dendrimer-encapsulated Au nanocluster decreases with decreasing the nanocluster size.

Figure 3 shows the Au $4f$ core-level XPS spectra of dendrimer-encapsulated Au nanoclusters supported on the HOPG substrate. The Au $4f$ core-level photoemission spectrum observed for bulk Au polycrystalline is also shown for a comparison. (Fig. 3a) Au $4f$ core level spectrum of dendrimer-encapsulated Au nanoclusters with diameter less than 1.0 nm shows similar spectral feature with that of bulk Au crystallite, while dendrimer-encapsulated Au nanoclusters with the mean diameter of 2.4 nm shows asymmetric spectral shape in the higher binding energy side. In order to discuss the detailed spectral features, we carried out the line shape analyses of Au $4f$ core-level photoemission spectra by a least-square method. The detailed procedure of these line shape analysis for Au $4f$ core-level spectra has been described elsewhere [7,8]. As previously well established, Au $4f$ core-level photoemission spectrum of Au bulk crystallite consists of two components, which originate from atoms in the bulk (bulk component) and surface atom layer (surface component). As shown in Figure 3a, it is found that the present Au $4f$ photoemission spectrum of bulk Au crystallite is also well reproduced by two components. The components in the higher binding energy and lower binding energy are assigned to bulk component (solid line) and surface component (dashed line), respectively, and the observed surface core-level shift of -0.29 eV is consistent with the literature values [8,9]. As shown in Figure 3b, it is found that the $4f$ core-level photoemission spectrum of dendrimer-encapsulated Au nanocluster with diameter of 2.4 nm is reproduced by the three components. The lowest-binding-energy component is assigned to bulk component, since the spectral feature and binding energy of the lowest-binding-energy component (solid line) is similar to that of bulk component in the Au $4f$ core-level spectrum observed for bulk Au crystallite. The lower energy component that observed for Au $4f$ core-level photoemission spectrum of bulk Au has not been observed. Since the diameter of dendrimer used in this study is about 3 nm, it is considered that Au nanocluster with the mean diameter of 2.4 nm would not be encapsulated within the internal spaces of the dendrimers. These clusters are stabilized by terminal groups on the dendrimer periphery. Therefore, these two higher-energy components (dotted lines) are considered to correspond to the surface components that originate from the termination with the terminal groups on the dendrimer periphery. These

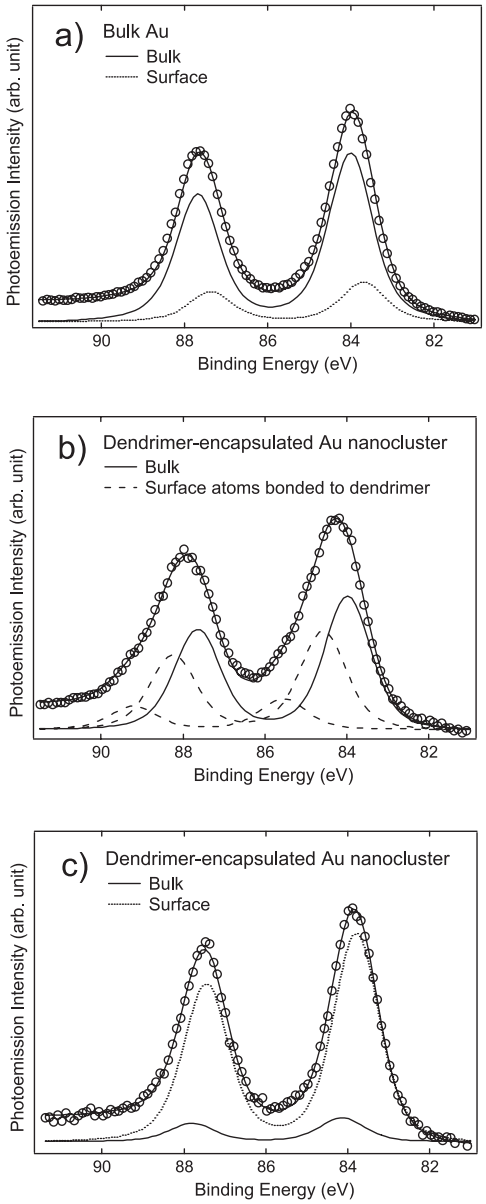

Fig. 3. Au $4f$ core-level X-ray photoemission spectra and the results of line-shape analyses of Au bulk crystallite (a) and dendrimer-encapsulated Au nanoclusters supported on the HOPG substrates (b and c) measured with the Mg$K\alpha$ line ($h\nu = 1253.6$ eV). The observed spectra of (a) bulk Au and (c) Au nanocluster with diameter less than 1.0 nm are decomposed into bulk components (solid lines) and surface components (dotted lines), and that of (b) Au nanocluster with mean diameter of 2.4 nm are decomposed into bulk components (solid line) and surface components (dashed line) terminated with the dendrimer.

surface components accompany with a chemical shift to higher binding-energy side. This means that the chemical states in the interface Au atoms terminated with the dendrimer is different with the inner Au atoms, and existence of a chemical reaction (chemisorption) between Au nanocluster and the carboxylate terminal groups on the dendrimer periphery. That is, the charge transfer occur from

Au nanocluster to carboxylate terminal groups on the dendrimer periphery. On the other hand, as shown in Figure 3c, it is found that the photoemission spectrum of dendrimer-encapsulated Au nanoclusters with the diameter less than 1.0 nm is reproduced by the two components fairly well. The binding energies and spectral features of these two components are quite similar to those of the bulk and surface components in the Au $4f$ core-level photoemission spectrum observed for the bulk Au crystallite. Therefore, it is considered that the components with higher binding-energy and lower binding-energy in the Au $4f$ core-level photoemission spectrum of the dendrimer-encapsulated Au nanoclusters with the diameter less than 1.0 nm corresponds to the inner atoms of Au nanoclusters (bulk component) and the surface Au atoms of Au nanoclusters (surface component), respectively. The much higher intensity of lower energy component compared with higher energy component is attributed to the higher relative number of surface to inner atoms. The absence of the spectral feature with chemical shift in the core-level spectra of dendrimer-encapsulated Au nanoclusters with the diameter less than 1 nm implies that Au nanoclusters are stabilized and isolated by the dendrimer without chemical interaction. It is concluded that cluster-size dependent $4f$ core-level photoemission spectra reflect the difference of the chemical states among the Au nanoclusters surface-terminated with dendrimers and dendrimer-encapsulated ones.

4 Conclusion

We have carried out the optical spectroscopic and XPS studies of two kinds of dendrimer-encapsulated Au nanoclusters with different size distributions. From the photoluminescence measurement, the synthesized dendrimer-encapsulated Au nanocluster with diameter less than 1.0 nm shows a strong blue photoluminescence around 2.8 eV photon energy. The photoluminescence from dendrimer-encapsulated Au nanocluster with diameter less than 1.0 nm is attributed to the new visible optical transition that results from the change of electronic structure due to quantum confinement. It is found that the apparent spin-orbit splitting of Au $5d$-derived band in the valence-band photoemission spectrum decreases with decreasing the nanocluster diameter. This originates from band-broadening contribution to the apparent spin-orbit splitting decreases with decreasing the nanocluster size, since the relative number of surface to inner atoms in nanocluster increases with the decreases of the nanocluster diameters.

Furthermore, we have observed Au $4f$ core-level photoemission spectrum of dendrimer-encapsulated Au nanoclusters. From the detailed line shape analyses, the cluster-size dependent $4f$ core-level photoemission spectra of dendrimer-encapsulated Au nanoclusters are observed. It is concluded that these cluster-size dependent Au $4f$ core-level spectra originates from the difference of chemical states among the Au nanoclusters surface-terminated with dendrimers and dendrimer-encapsulated ones.

This work was supported by Grant-in-Aids from the Ministry of Education, Culture, Sports, Science and Technology (MEXT) of Japan. This work was also supported by the grants from Hyogo Science and Technology Association and Kawanishi Memorial Shinmaywa Education Foundation. A part of this work was performed under "Nanotechnology Support Project" of MEXT, Japan.

References

1. M.J. Hostetler, J.E. Wingate, C. Zhong, J.E. Harris, R.W. Vachet, M.R. Clark, J.D. Londono, S.J. Green, J.J. Stokes, G.D. Wignall, G.L. Glish, M.D. Porter, N.D. Evans, R.W. Murray, Langmuir **14**, 17 (1998)
2. M. Alvarez, J.T. Khoury, T.G. Shaaff, M.N. Shafigullin, I. Vezmar, R.L. Whetten, J. Phys. Chem. **101**, 3706 (1997)
3. Y.G. Kim, J.C.G. Martinez, R.M. Crooks, Langmuir **21**, 5485 (2005)
4. J. Zheng, C. Zhang, R.M. Dickson, Phys. Rev. Lett. **93**, 077402 (2004)
5. T. Endo, T. Yoshimura, K. Esumi, Coll. Int. Sci. **269**, 364 (2004)
6. A. Bzowski, T.K. Sham, R.E. Watson, M. Weinert, Phys. Rev. B **51**, 9979 (1995)
7. A. Tanaka, Y. Takeda, M. Imamura, S. Sato, Phys. Rev. B **59**, 195415 (2003)
8. A. Tanaka, Y. Takeda, T. Nagasawa, K. Takahashi, Solid State Commun. **126**, 191 (2003)
9. T.C. Hsieh, A.P. Shapiro, T.C. Chiang, Phys. Rev. B **73**, 3160 (1983)